Multicomponent Analysis of Strong Lensing Galaxy Clusters as an Observational Test of Cosmological Structure Predictions

Raven Gassis

University of Cinncinnati

mm Universe 2023

June 26th, 2023

Background I

- Galaxy clusters form by the gradual accretion of many mass halo systems.
- Brightest Cluster Galaxy (BCG) shares halo orientation and centroid.
- Intracluster Light (ICL) and Intracluster Medium (ICM) should trace out halo shape and share its centroid.
- The Core Lensing Mass derived from strong lensing mass models can tightly constrain halo mass distribution.

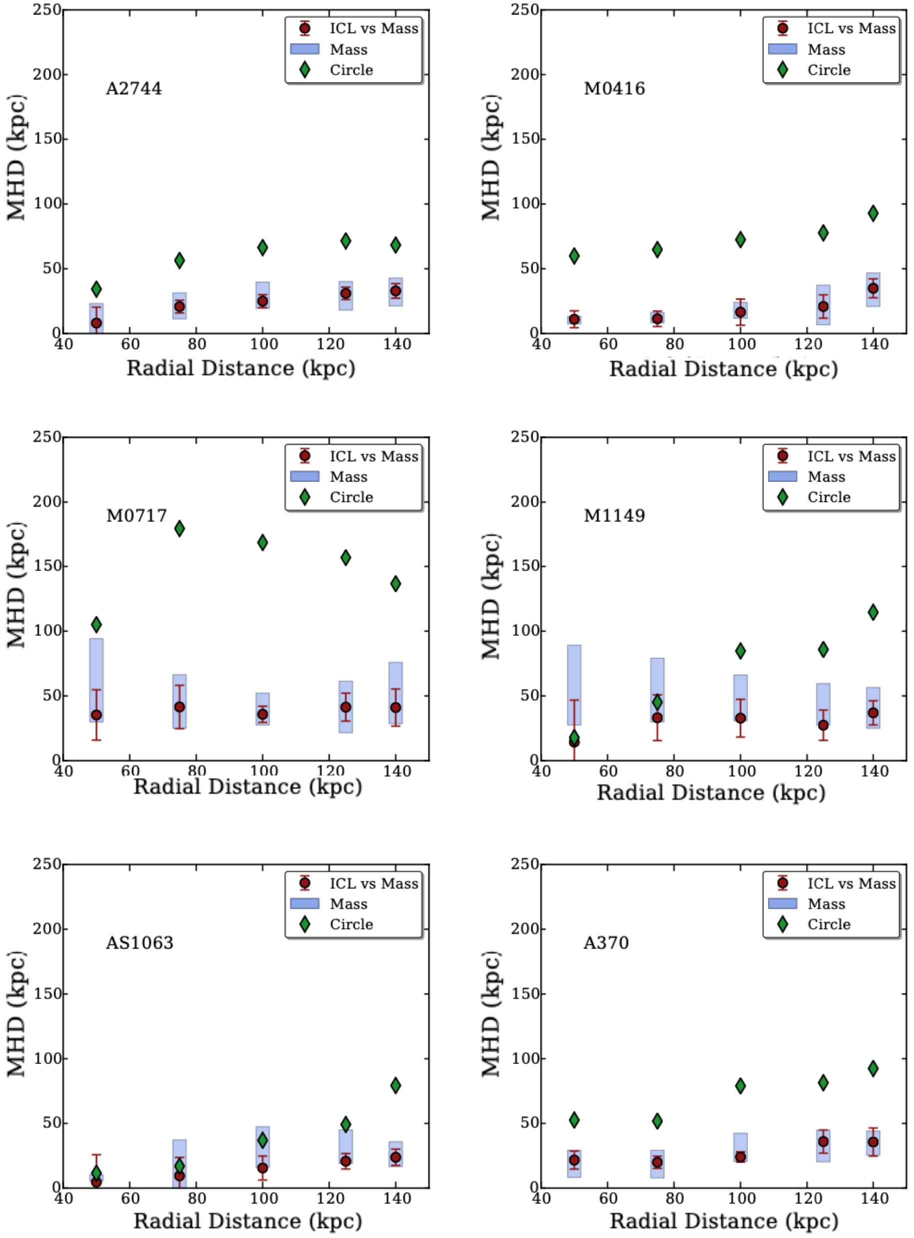

Figure 1: From Montes & Trujillo 2018: Graphic showing the ability of the ICL to trace out the matter potential using the Modified Hausdorff Distance (MHD) between the ICL and gravitational lensing mass models.

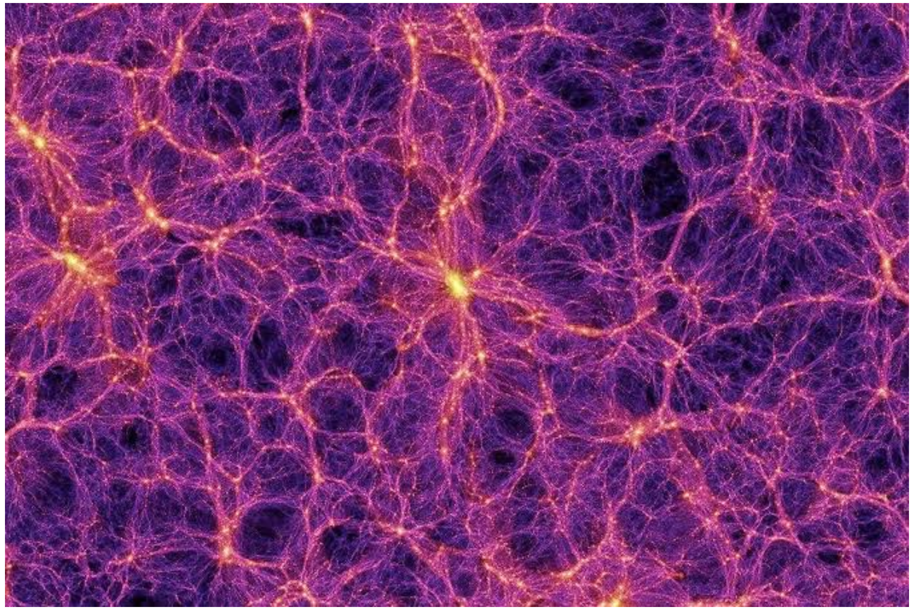

Figure 2: From Volker Springel / Max Planck Institute For Astrophysics. Data Visualization of Cosmic Web From the Millennium Simulation

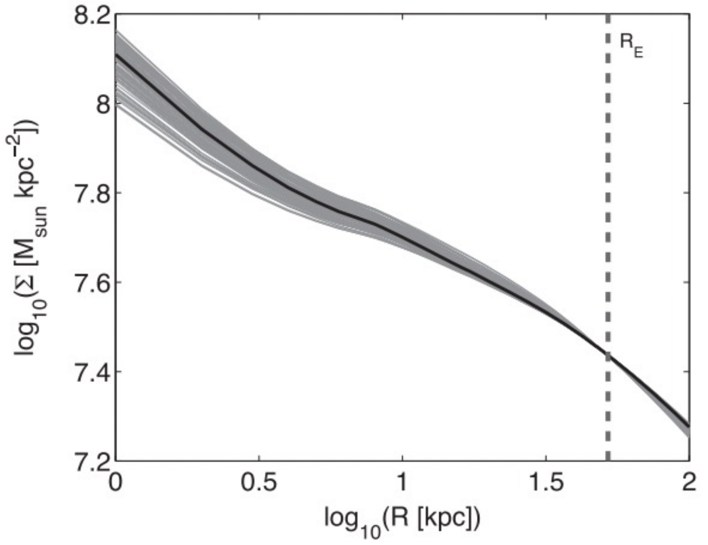

Figure 3: From Sharon et al. 2014. the mass profile of example cluster SDSSJ1531+3414.

Background II

- Based on ΛCDM, the BCG, ICL, and ICM should all align with the Core Lensing Mass of the cluster halo.

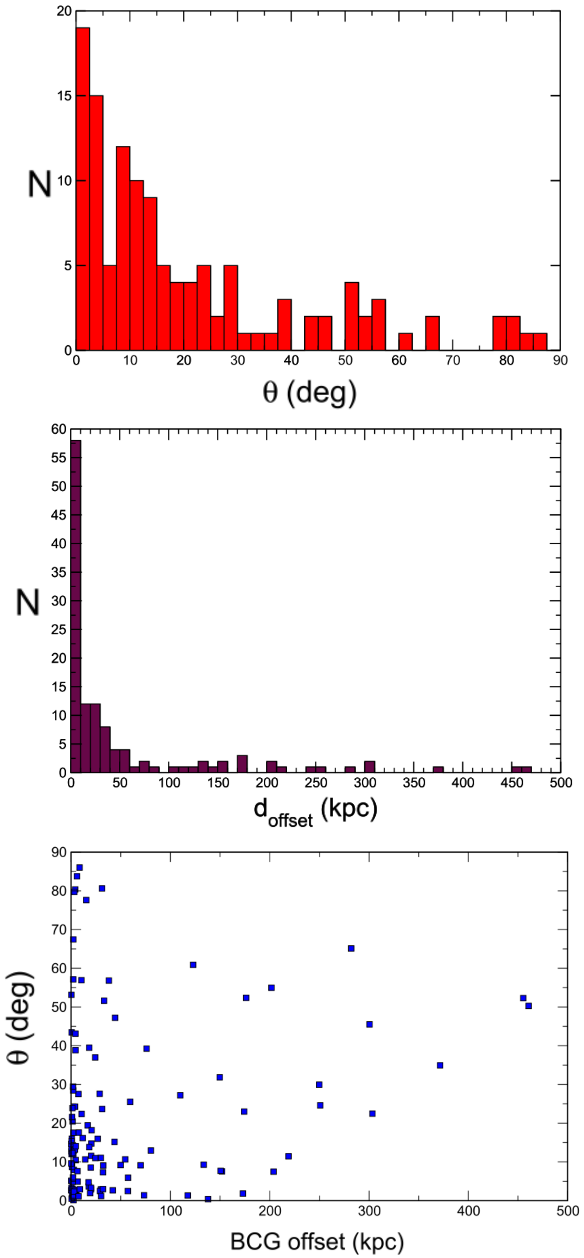

Figure 4: From De Propris et al. 2021 comparing the BCG and X-ray ICM.

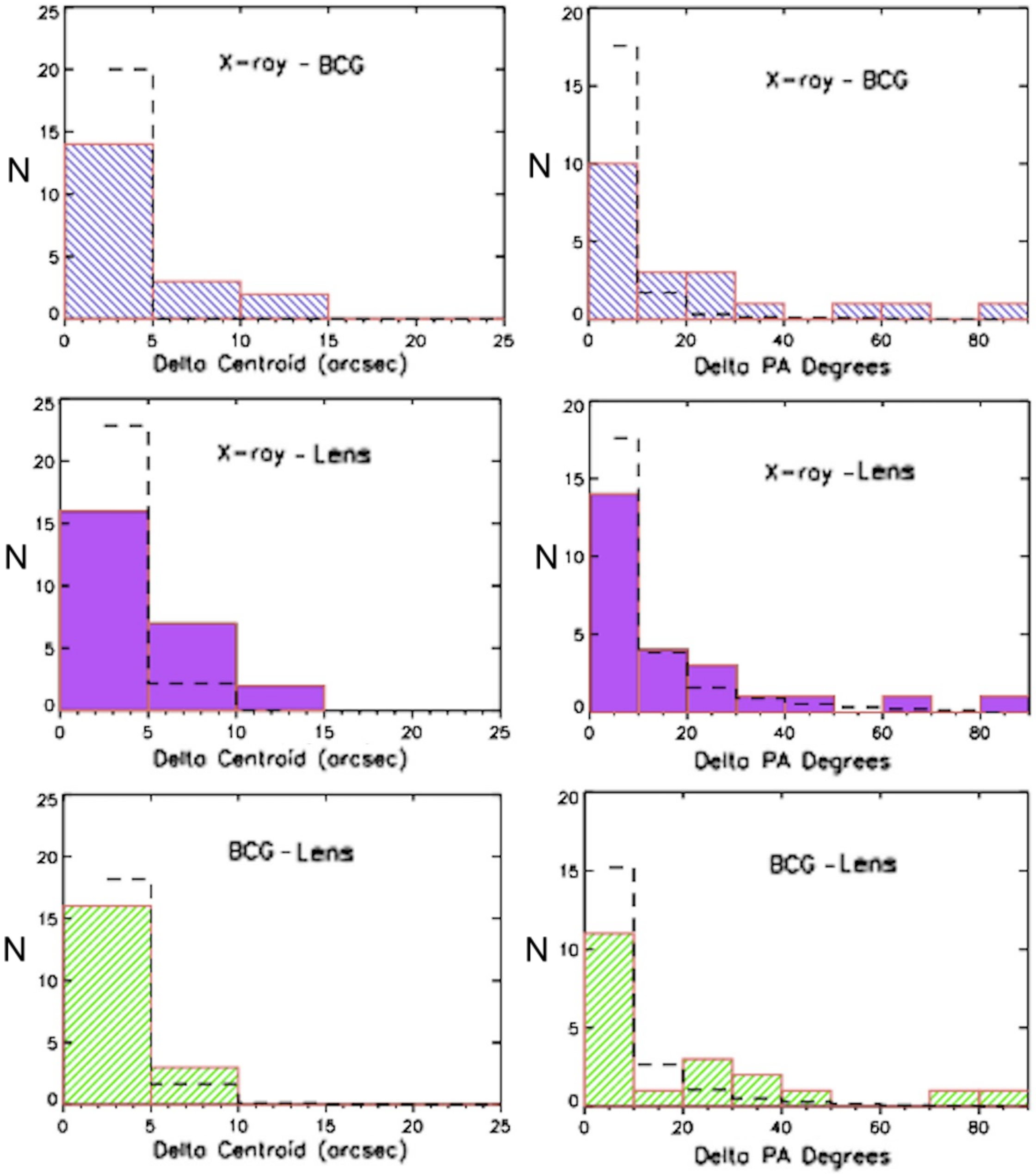

Figure 5: From Donahue et al. 2016: Plot showing the difference in position angle and centroids for various components of galaxy clusters.

Background II

- Based on ΛCDM, the BCG, ICL, and ICM should all align with the Core Lensing Mass of the cluster halo.

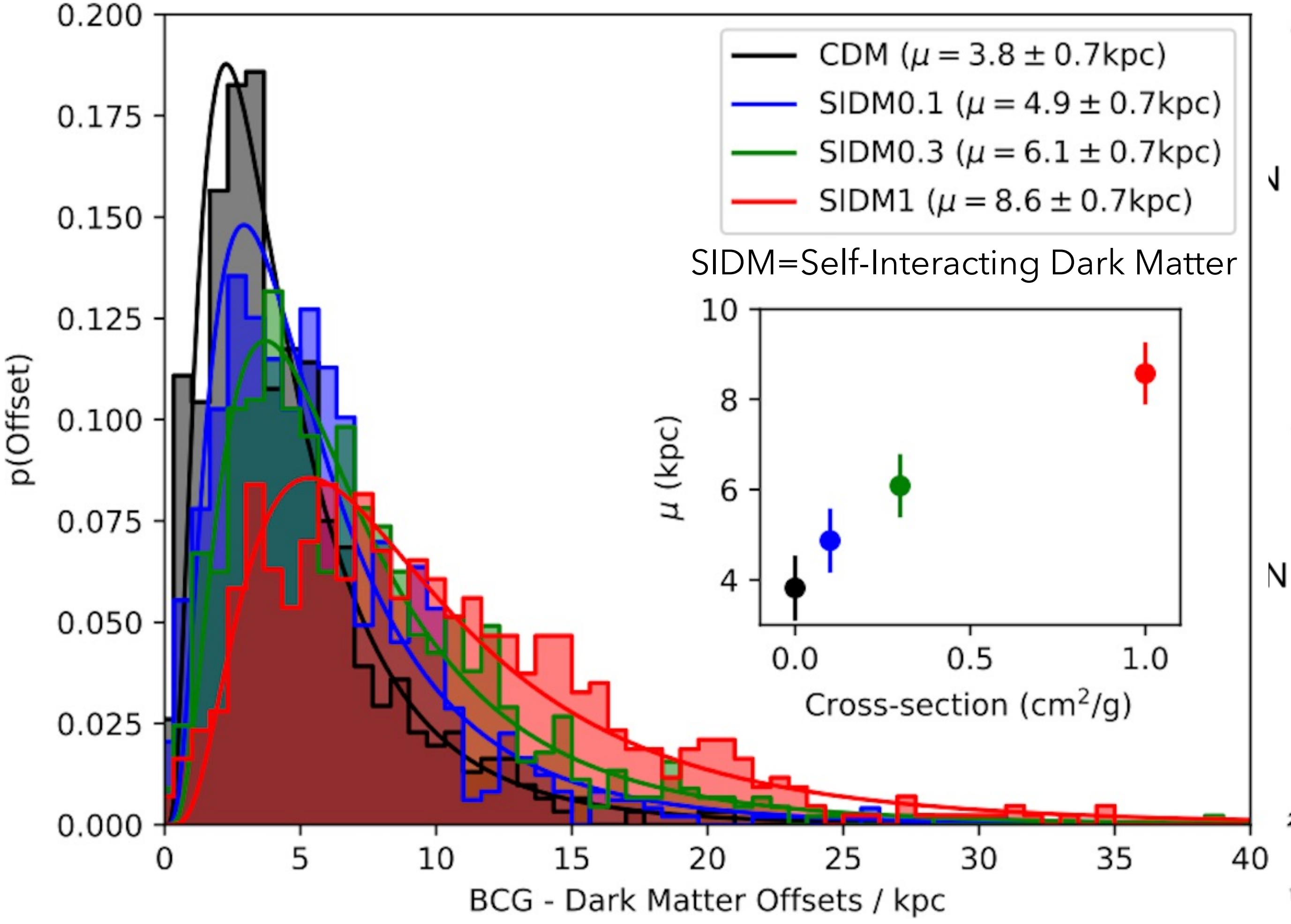

Figure 6: From Harvey et al. 2019: showing the spatial offset between the BCG and dark matter halo for different dark matter cross-sections with a lognormal distribution fitted to each sample.

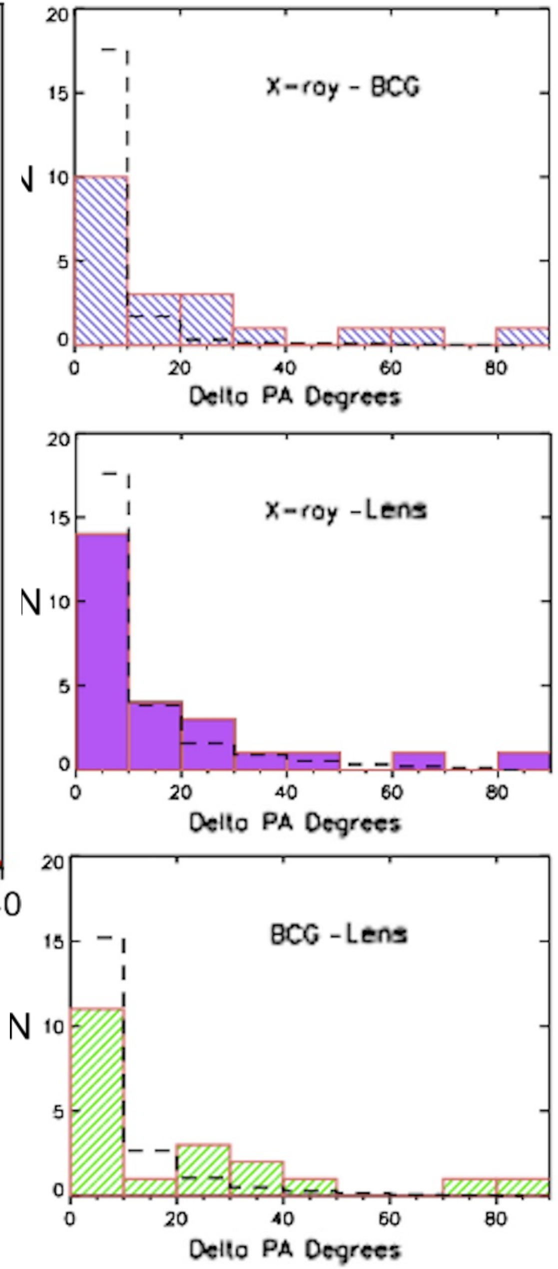

Figure 4: From De Propris et al. 2021 comparing the BCG and X-ray ICM.

Figure 5: From Donahue et al. 2016: Plot showing the difference in position angle and centroids for various components of galaxy clusters.

Raven Gassis, mm Universe 2023

The Data I: Strong Lensing Sample and HST Data

- We select our clusters from the Sloan Giant Arcs Survey, SGAS (Koester et al. 2010; Bayliss et al. 2011, 2014; Gladders et al. 2013)
- The sample is strong lensing selected with corresponding mass models (Sharon et al. 2020, 2022a, 2022b)

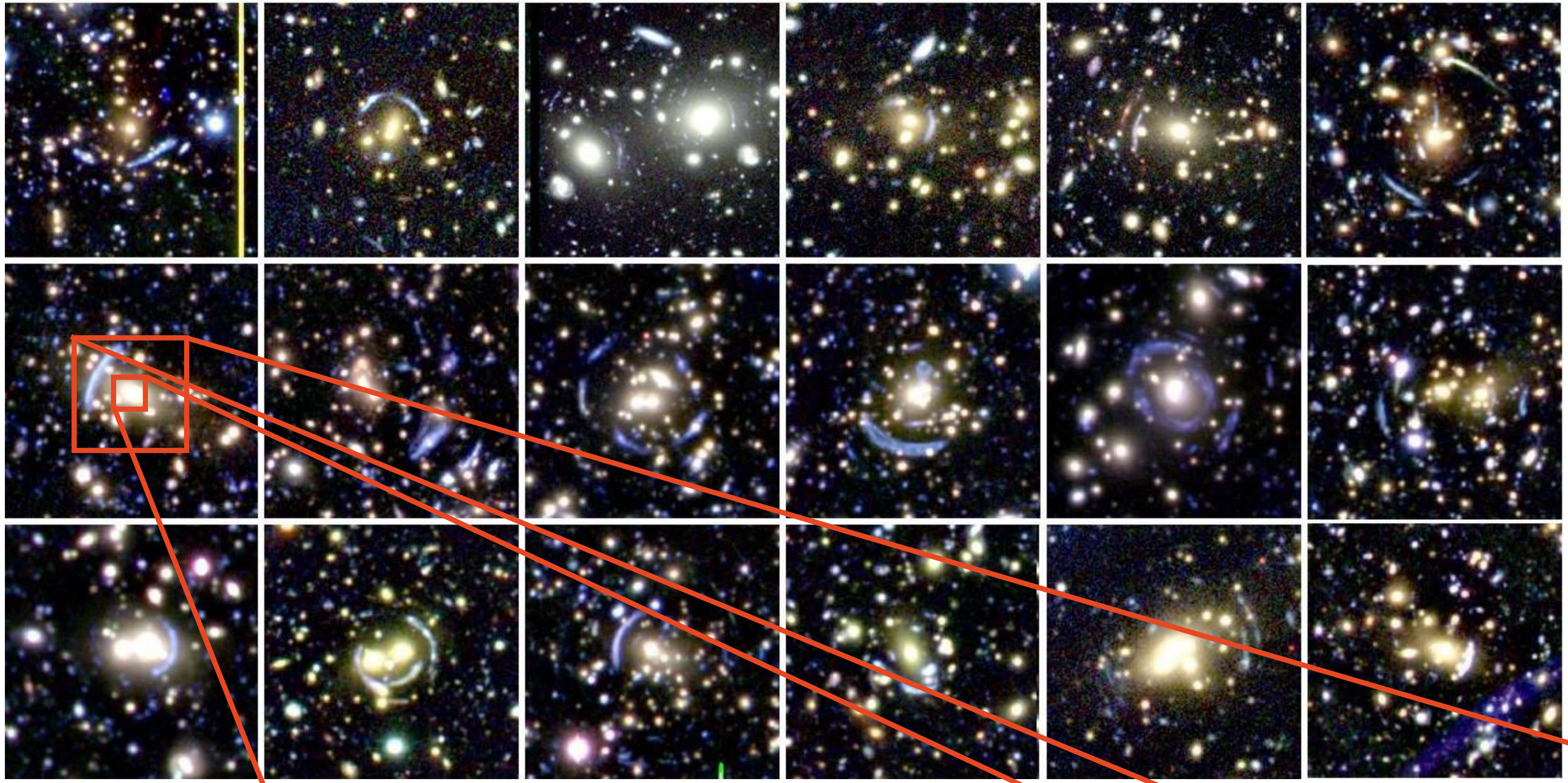

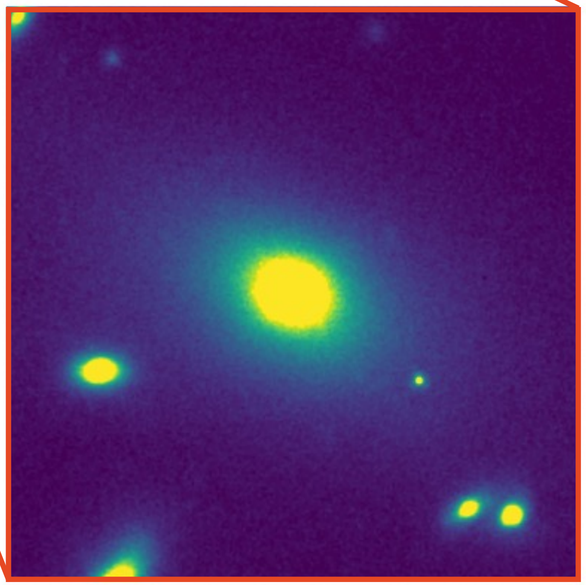

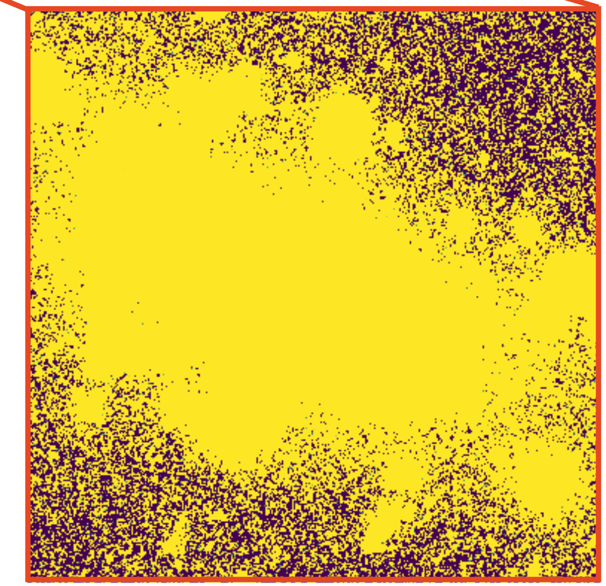

Figure 8: Color images of a subsample of our strong lensing selected cluster sample with WFC3/IR HST F160W *zoom-ins for example cluster* J1343p4155.

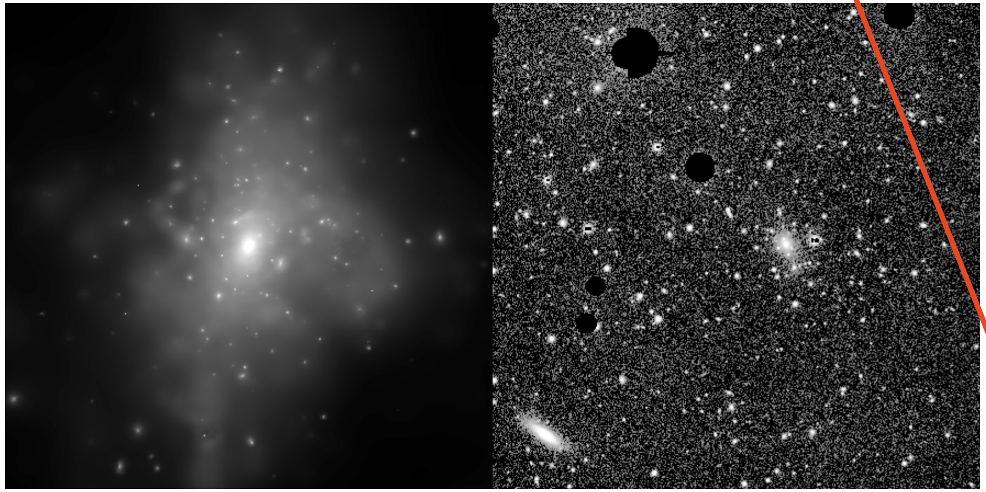

Figure 7: From a Fermilab news article written by S. Koppes. Shows IllustrisTNG simulation data (Jesse Golden-Marx) and the Dark Energy Survey cluster data (DES and Yuanyuan Zhang)

Data II: Chandra Data

- ICM Measurements are made using Chandra ACIS-I Data.
- X-ray data allows us to make additional measurements on the dynamical state of the galaxy cluster

Figure 9: Adaptively smoothed Chandra Data for a subsample of our strong lensing cluster. sample.

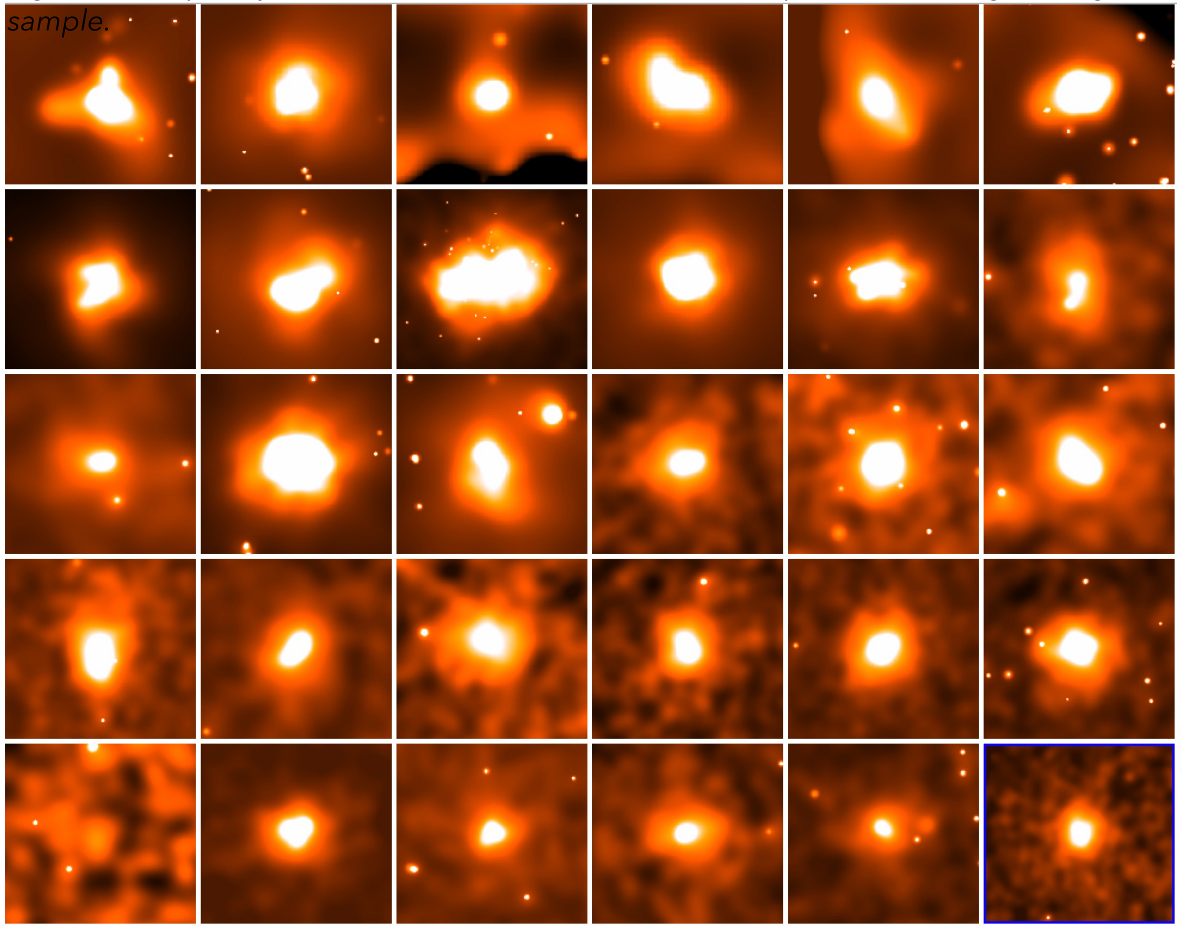

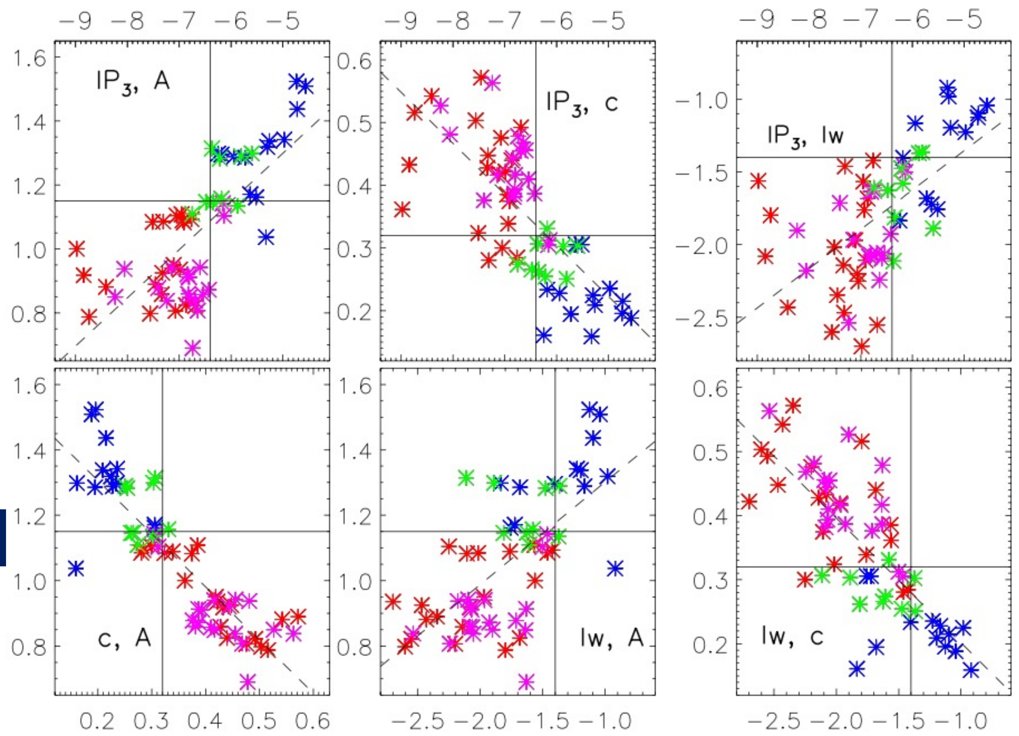

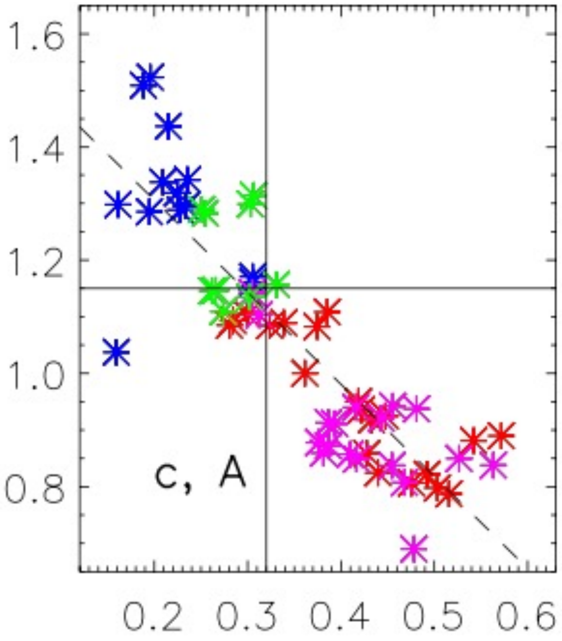

par pairs	L ver.	L hor.	regular P_r	regular C_r	disturbed P_d	disturbed C_d
$\log_{10}(P_3), A$	-6.4	1.15	0.95	0.95	1.0	0.77
$\log_{10}(P_3), c$	-6.4	0.32	1.00	0.87	0.9	0.45
$\log_{10}(P_3), \log_{10}(w)$	-6.4	-1.4	0.95	0.95	1.0	0.45
c, A	0.32	1.15	1.00	0.87	1.0	0.72
$\log_{10}(w), A$	-1.4	1.15	0.93	1.00	1.0	0.36
$\log_{10}(w), c$	-1.4	0.32	0.97	0.87	1.0	0.45
$A_{\rm rot}, F$	1.15	1.00	0.89	0.89	1.0	0.83

Figure 10 and Table 1: Adapted from Rasia et al. 2013. Plots of various relaxation parameters compared to one another. In the figure, red, blue, green and magenta points denote regular, disturbed, semi-regular, and semi-disturbed clusters. The table highlights the completeness and purity of measured relaxed/disturbed clusters as well as gives the cut-values for dynamical state for each parameter

Measurement methods

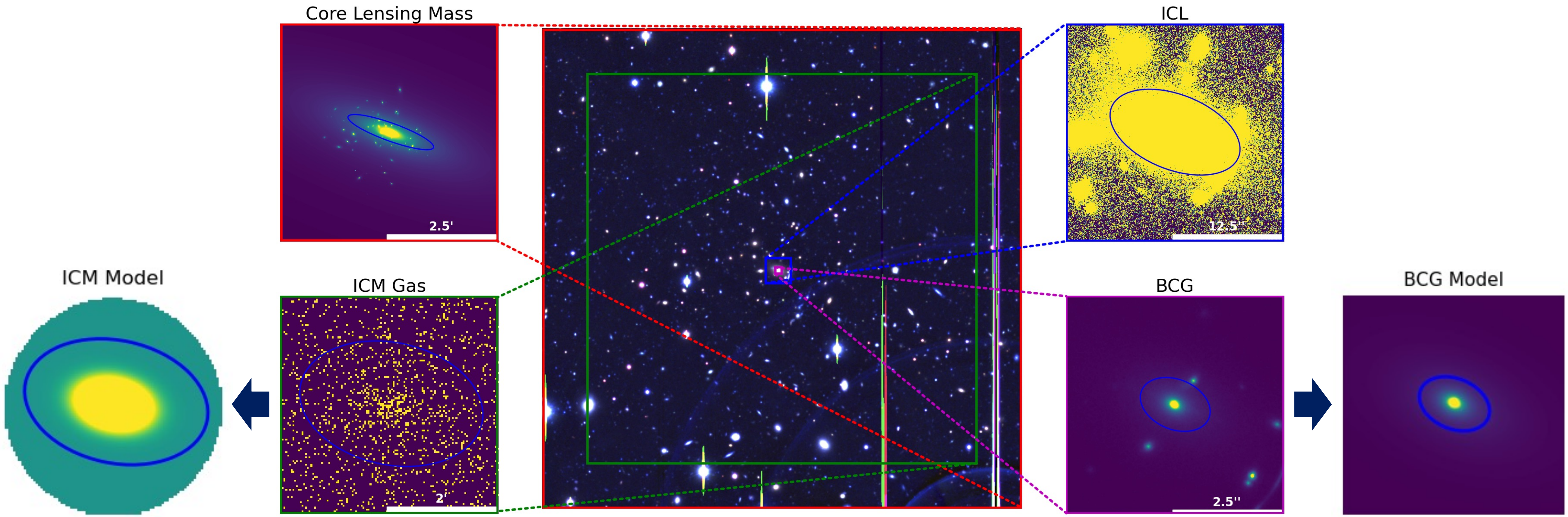

Figure 11: Visualization of the data distributions with the corresponding best fit ellipse for example galaxy cluster J0957p0509

Results I: Position Angles

- Generally, we measure small position angle differences which implies that cluster orientation is consistent over a large spatial scale (from 10s of kpc to ~1 MPC).
- The percentage of high position angle differences (ΔPA > 30°) is 39%, 34%, and 26% for the core lensing mass-BCG, core lensing mass-ICM, and core lensing mass-ICL comparisons respectively.
- The small number of misalignments between the ICL and core lensing mass suggests that the ICL may be a more viable proxy for the shape and orientation of the dark matter halo distribution in many cases.

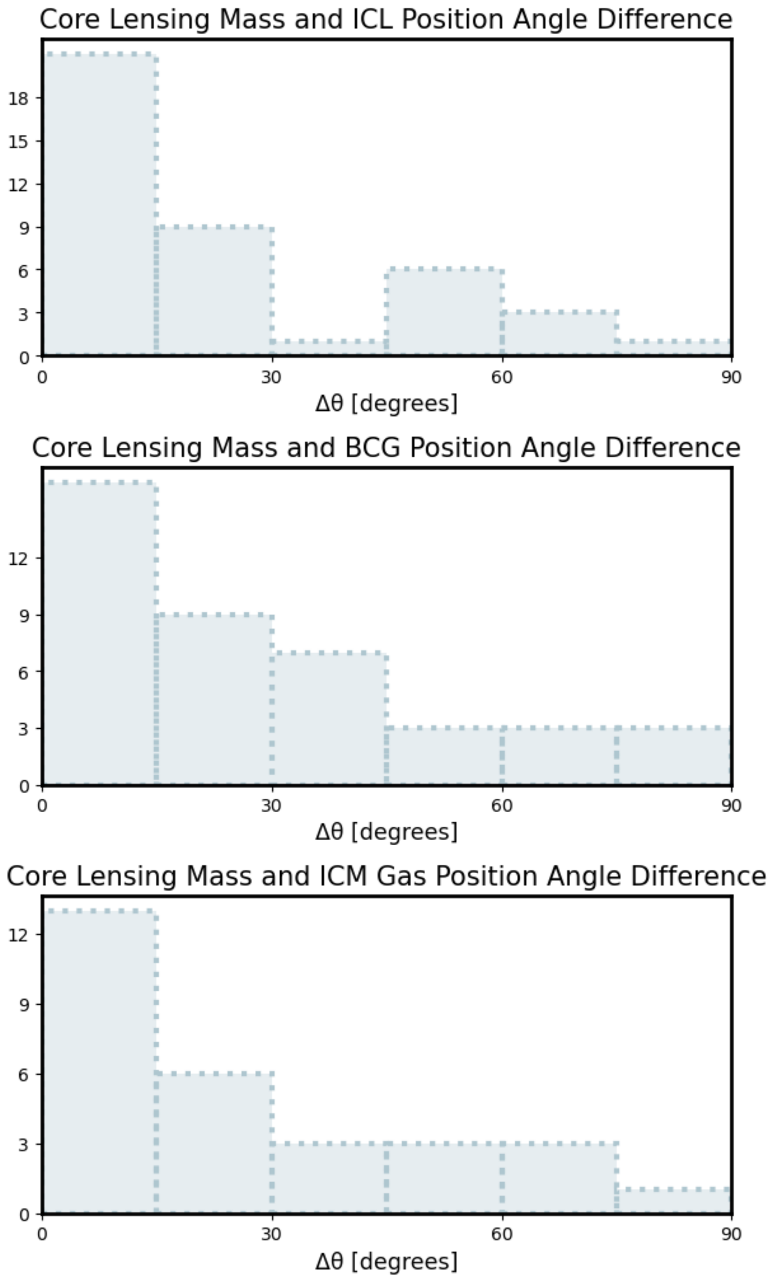

Figure 12: The difference in position angle of the major axis between the core lensing mass and the three other distributions (from top to bottom: ICL, BCG, and ICM)

Results II: Ellipticities

- BCGs likely tend to have smaller ellipticities due to dynamical friction effects as a consequence of high stellar density
- The dark matter and stellar distribution characterized by the ICL trace out the same shape with a large amount of scatter.
- The ICM is generally more round than the dark matter and stellar distributions. This likely reflects the effects of hydrodynamical physics in the ICM.

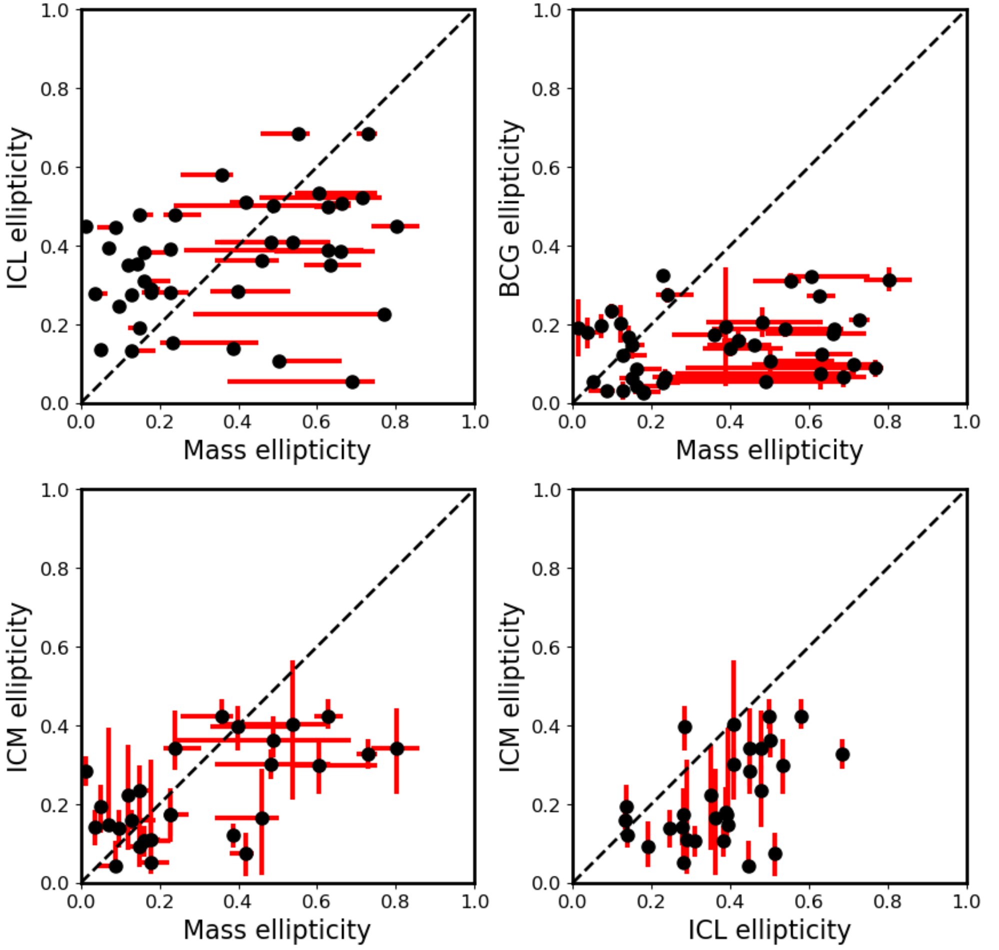

Figure 13: the ellipticity comparisons of various distributions (top-left: core lensing mass and ICL, top-right: core lensing mass and BCG, bottom-left: core lensing mass and ICM, bottom-right: ICL and ICM)

Results III: Dynamical Analysis

- Folding in dynamical state and spatial offset can give possible explanations for high position angle difference for sufficiently elliptical distributions
- We use ΔPA > 30° to define a large position angle difference and ellipticity > .1365 to define a well defined ellipticity for all components measured.
- For clusters that fall into the definition of well-defined ellipticity and large position angle difference 60%,80%,and 50% are disturbed or in an undefined state for the BCG, ICM, and ICL respectively.

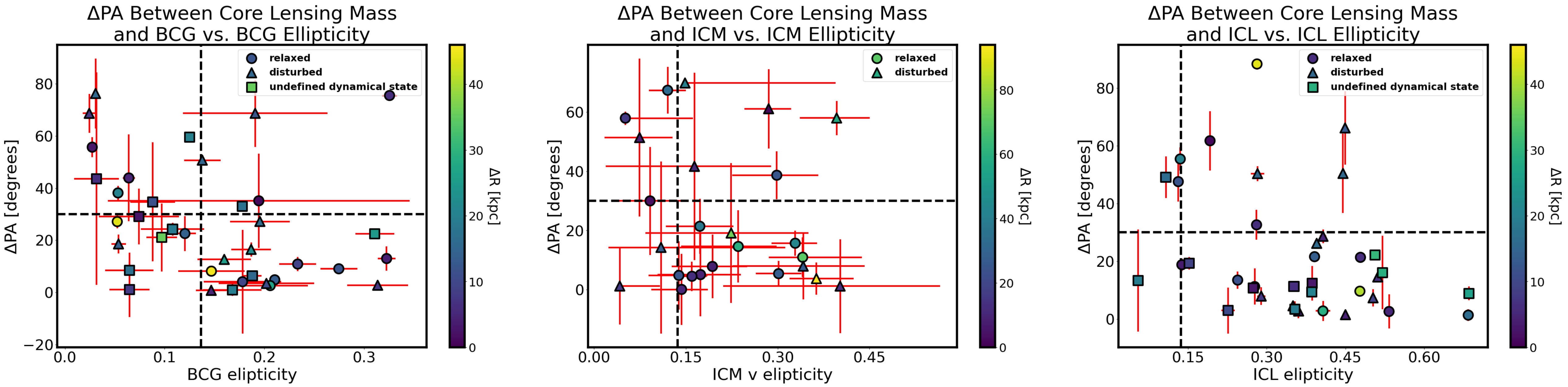

Figure 14: The position angle difference between the Core Lensing Mass and another physical component's distribution as a function of that component's ellipticity with radial offset of the centroids indicated by the color (components from left to right: BCG, ICM, ICL). The dynamical states are indicated by the markers (circle=relaxed, triangle=disturbed, square=undefined dynamical state)

Results IV: Centroids

- We typically measure small deviations for the BCG and ICL distributions with respect to the core lensing mass.
- The ICL and BCG are typically displaced in tandem with one another but the BCG exhibits greater displacement generally.
- The ICM has the greatest deviations from the core lensing mass likely due to ICM Gas "sloshing" as a consequence of hydrodynamic processes.

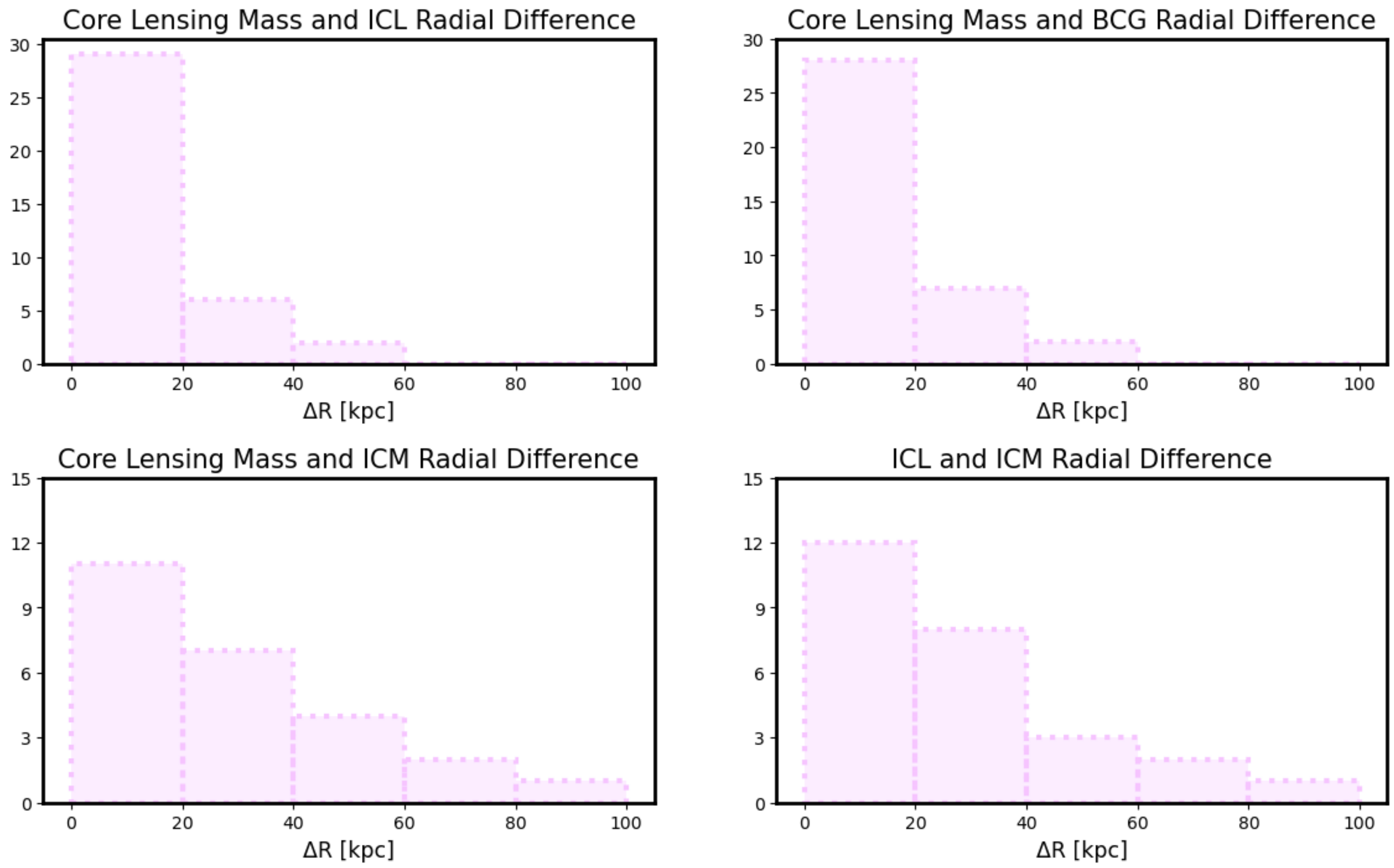

Figure 15: The comparison of centroid deviation in kpc of various components of our galaxy cluster systems. We compare the centroids of the ICL and Core Lensing Mass (top-left), the BCG and the Core Lensing Mass (top-right), the ICM Gas and the Core Lensing Mass (bottom-left), and the ICM Gas and ICL (bottom-right). For the the ICM Gas and ICL histogram, we ignore double cored systems undergoing an obvious major merger event.

Conclusions

- Generally, we find that strong lensing galaxy clusters show good alignment with Lambda CDM predictions and can explain misalignments with astrophysical phenomena (BCG circularization, hydrodynamical sphericalization, dynamical disruptions, etc.)
- Misalignments do however occur beyond expectation suggesting a high frequency of these astrophysical phenomena or potentially other explanations within or beyond the context of ΛCDM.
- The BCG and ICM are more spherical than the ICL leading to a higher frequency of misalignments in orientation.
- The ICM is subject to hydrodynamical effects that lead to higher frequency of spatial offsets than the other components.
- The ICM is more intensely affected by dynamical disruptions.

Overflow

Physical Construction

- Typically, we measure large position angle differences in cases where either the BCG is circularized or has a offset centroid with respect to the core lensing mass.
- We recognize the same L-shaped behavior for the ICM.
- For the ICL, we see the best alignment with fewest cases of the ICL being offset in position angle and centroid space.

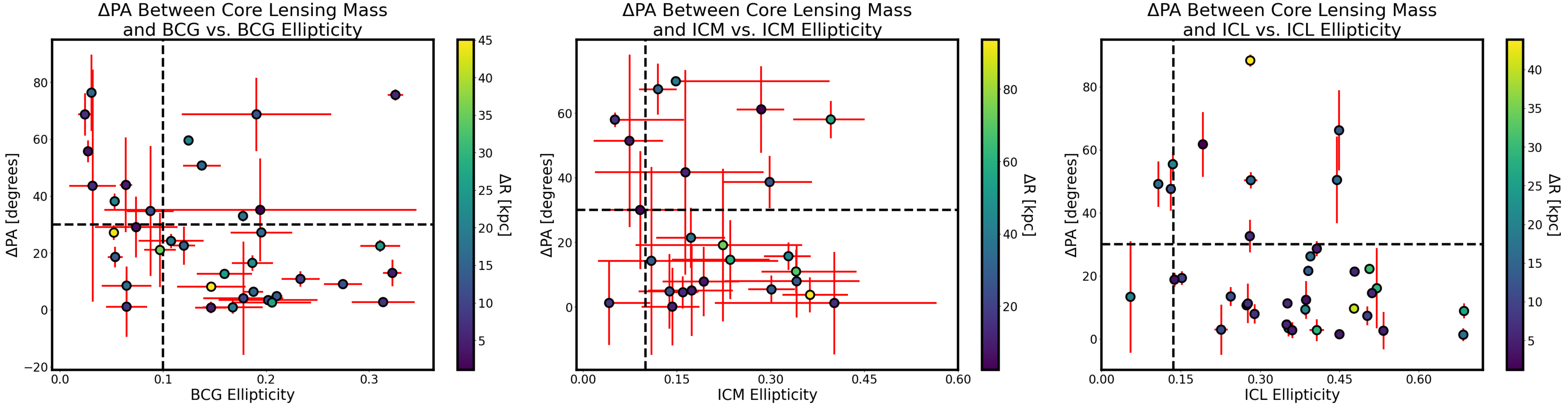

Figure 16: The position angle difference between the Core Lensing Mass and the another physical components distribution as a function of that components ellipticity with radial offset of the centroids indicated by the color. Middle: the position angle difference between the Core Lensing Mass and the ICM distributions as a function of ICM ellipticity with radial offset of the centroids indicated by the color. Right: the position angle difference between the Core Lensing Mass and the ICL distributions as a function of ICL ellipticity with radial offset of the centroids indicated by the color. ΔPA = 30° and ellipticity=.1365 are highlighted by the dashed lines.

Dynamical Analysis I

- Often the BCG, ICL, and ICM are either disturbed or have an undefined dynamical state in cases where the ellipticity is relatively well defined and the position angle difference is relatively high.
- We use ΔPA > 30° to define a large position angle difference and ellipticity > .1365 to define a well defined ellipticity for all components measured.
- For clusters that fall into the definition of well-defined ellipticity and large position angle difference 60%,80%,and 50% are disturbed or in an undefined state for the BCG, ICM, and ICL respectively.

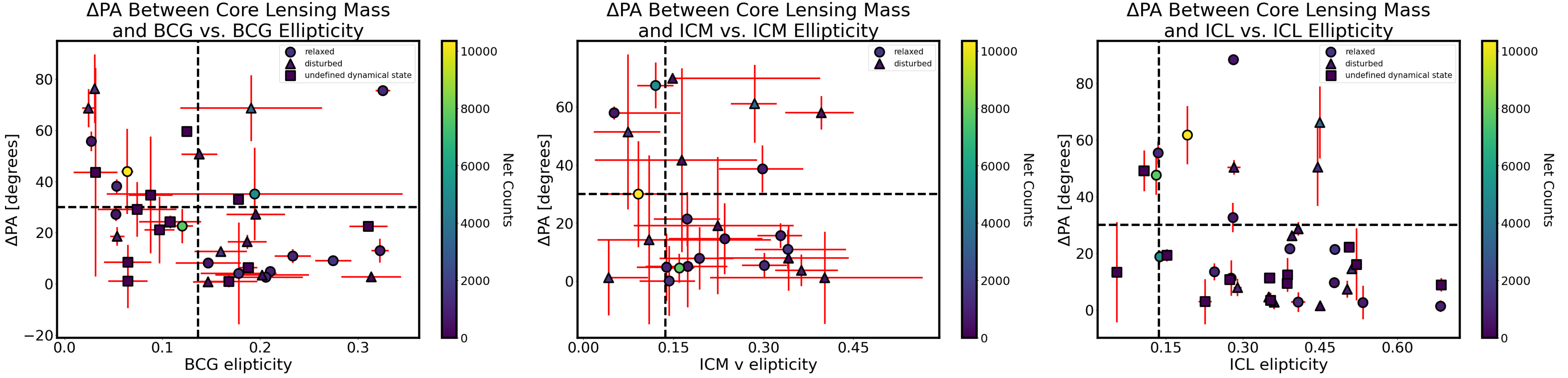

Figure 17:Left: the position angle difference between the Core Lensing Mass and the BCG distributions as a function of BCG ellipticity. Middle: the position angle difference between the Core Lensing Mass and the ICM distributions as a function of ICM ellipticity. Right: the position angle difference between the Core Lensing Mass and the ICL distributions as a function of ICL ellipticity. In each graph, color indicates number of counts of the X-ray data. For objects with no X-ray data and undefined dynamical states we set net counts to 0. We distinguish points by their dynamical state: circles indicating relaxed clusters, triangles indicating disturbed clusters, and squares indicating an unknown dynamical state. ΔPA = 30° and ellipticity=.1365 degrees are highlighted by the dashed lines

Dynamical Analysis II

- Somewhat unexpectedly, for both the BCG and ICL distributions, a high percentage of relaxed clusters have spatial deviations over 20kpc.
- We observe the BCG and ICL are simultaneously misaligned with the core lensing mass centroid in relaxed clusters
- In disturbed clusters with high spatial deviations, it seems that the BCG is displaced while the ICL remains aligned.
- The ICM gas exhibits the expected behavior in that disturbed clusters are more misaligned than the relaxed clusters as a consequence of spatial disruptions due to mergers.

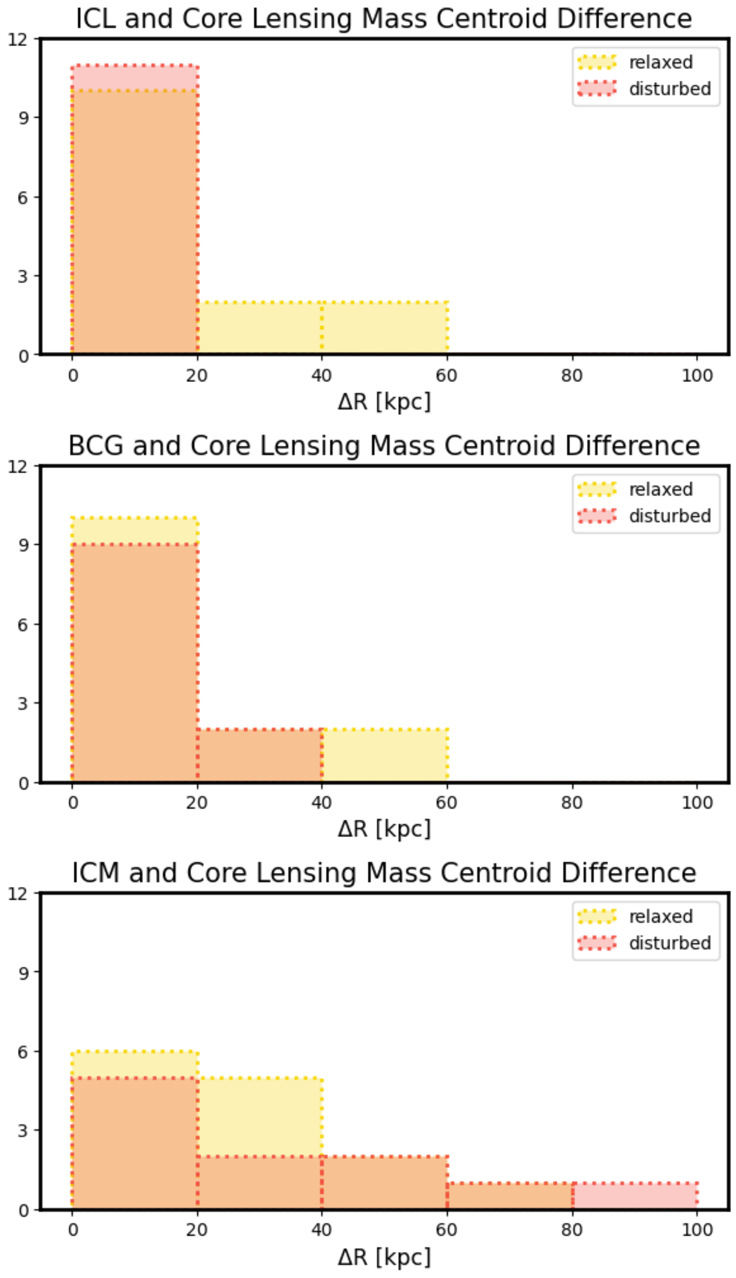

Figure 18: The comparison of centroid deviation in kpc of the ICL, BCG, and ICM gas (top to bottom) components of our galaxy cluster systems with respect to the Core Lensing Mass centroid. We only include systems where we have all 4 components measured simultaneously such that we are able to define the dynamical state using the ICM gas component. In these histograms, red indicates a disturbed dynamical state and yellow indicates a relaxed dynamical state.

Sample Motivation

- Selection based on strong Lensing cross section as opposed to a particular mass observable.
- Novel way to connect to simulations.

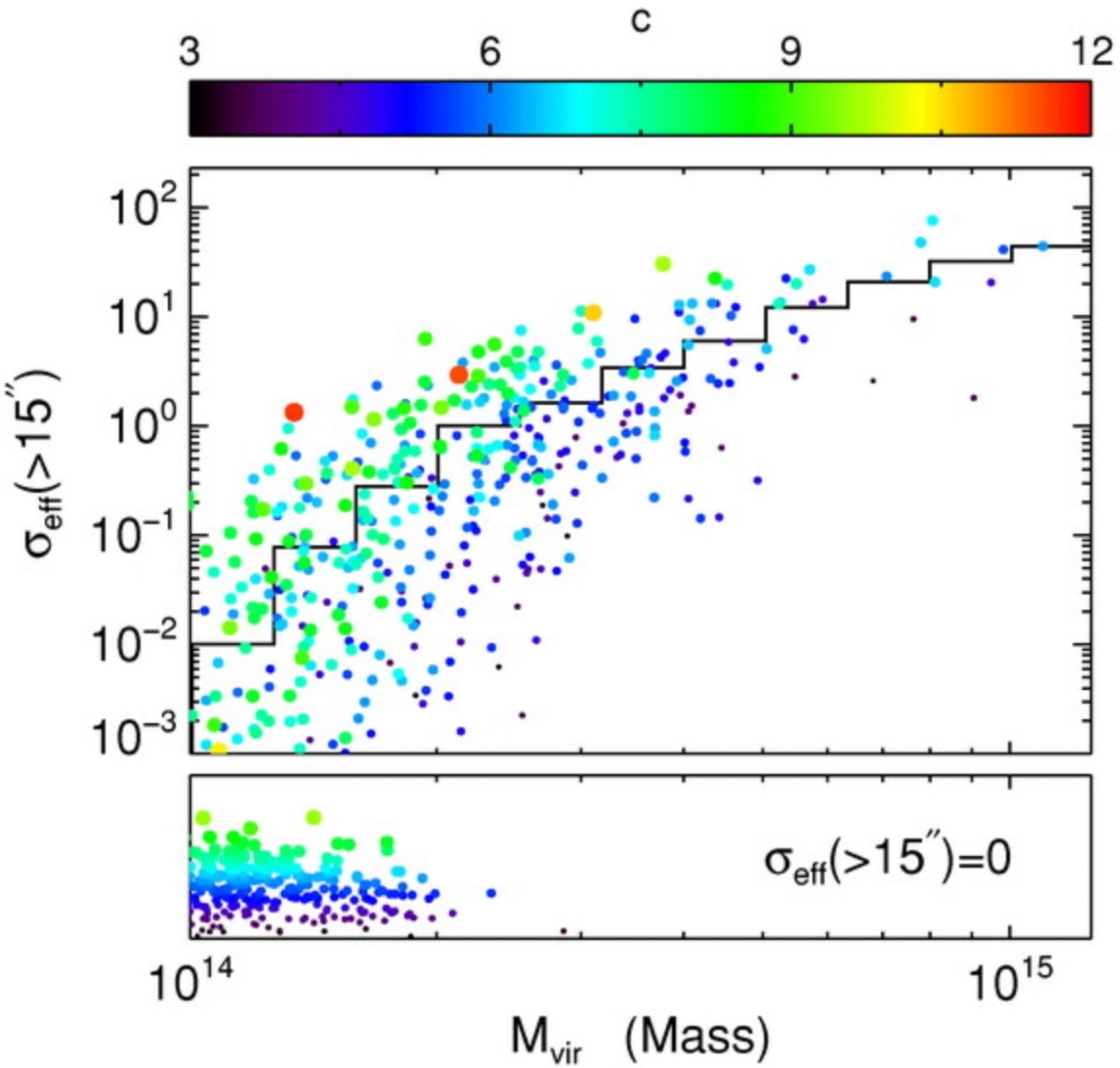

Figure 19: From Hinnawi et. al 2007. The distribution of clusters with strong lensing cluster to form arcs above 15" as a function of mass. c denotes the value of the lens strength parameter $\kappa_s = \rho_s r_s / \Sigma_s$